Transport model study of the m_T-scaling for Λ, K, and π HBT-correlations

Qingfeng Li [a,*], Marcus Bleicher [b], Horst Stöcker [a,b,c]

[a] *Frankfurt Institute for Advanced Studies (FIAS), Johann Wolfgang Goethe-Universität, Max-von-Laue-Str. 1, D-60438 Frankfurt am Main, Germany*
[b] *Institut für Theoretische Physik, Johann Wolfgang Goethe-Universität, Max-von-Laue-Str. 1, D-60438 Frankfurt am Main, Germany*
[c] *Gesellschaft für Schwerionenforschung, Darmstadt (GSI), Germany*

ARTICLE INFO

ABSTRACT

Based on the microscopic transport model UrQMD in which hadronic and string degrees of freedom are employed, the HBT parameters in the longitudinal co-moving system are investigated for charged pion and kaon, and Λ sources in heavy ion collisions (HICs) at SPS and RHIC energies. In the Cascade mode, R_O and the R_L at high SPS and RHIC energies do not follow the m_T-scaling, however, after considering a soft equation of state with momentum dependence (SM-EoS) for formed baryons and a density-dependent Skyrme-like potential for "pre-formed" particles, the HBT radii of pions and kaons and even those of Λs with large transverse momenta follow the m_T-scaling function $R = 3/\sqrt{m_T}$ fairly well.

In order to explore the properties of the fireball which is created just after the collision of two energetic nuclei, the Hanbury–Brown–Twiss interferometry (HBT) technique has been used and developed in astro- and nuclear-particle physics for about half a century. It is well known that the HBT technique can provide important information about the spatio-temporal structure of the particle emission source (the region of homogeneity). In [1], a non-trivial transition in the excitation function of spatio-temporal characteristics of the source was proposed. Meanwhile, the AGS, SPS and RHIC experiments (with nucleon–nucleon center-of-mass energies $\sqrt{s_{NN}}$ from about 2.5 GeV up to 200 GeV for heavy ion collisions) have been stimulating the HBT related investigations further into another golden era. Although the experiments have discovered quite a few exciting hints for a new phase of matter–maybe a quark gluon plasma (QGP) (see, e.g., Refs. [2,3]), a plethora of puzzling phenomena also came out. Examples related to HBT are

1. the discovered that there is no *obvious* peak/valley of the HBT quantities over the whole beam energies from SIS, AGS, SPS, up to RHIC as suggested in [1];
2. that hydrodynamic as well as transport (cascade mode) calculations show that the calculated ratio of the HBT radii in outward and sideward directions is higher than the experimental data, which is known as the HBT time-puzzle ("t-puzzle") [4–7]. For possible solutions of the "t-puzzle" we refer to [8–13];

3. mainly due to the resonance decay contribution of the particle production as well as the effects of strong and electromagnetic forces, the correlation function of identical particles deviates from a Gaussian type [4,14].

A "direct" study of the so-called "non-Gaussian effect"–the emission source image technique–has been quickly improving in recent years [15–18]. However, in order to theoretically investigate previous data and due to the fact that it gives a leading-order approximation to the real shape of the homogeneity region, the Gaussian parameterization is still important. During the process of Gaussian parameterization, it is known that on both experimental and theoretical sides, a proper potential modification of the final state interaction (FSI) after freeze-out should be analyzed before any work is done because of the intrinsic physical characteristic of correlated pairs. For example, charged pion–pion interferometry is only relatively weakly affected by the Coulomb and nuclear potentials due to its small mass and collision cross section, while for the charged kaon–kaon case, the Coulomb modification should be taken into account in the analysis [4,19]. For baryon–baryon correlation, a proper nuclear potential modification has to be considered. In the absence of FSI and from a hydrodynamic point of view in which the freeze-out of particles is flow-dominated, the HBT radii are predicted to decrease with $1/\sqrt{m_T}$ (m_T-scaling), m_T is the transverse mass of the observed particle-pair, independent of the particle species [20]. This prediction has been probed by recent experiments with energies from AGS to RHIC. In Ref. [21], an m_T-scaling expression $3/\sqrt{m_T}$ has been suggested at $E_{lab} = 158\,A$ GeV. It is also supported by other experiments at RHIC energies (see references in, e.g., [4]). However, due to the lack of data and the

* Corresponding author.
E-mail address: liqf@fias.uni-frankfurt.de (Q. Li).

rather large experimental errors, a firm conclusion is still awaiting. It is also urgent to perform microscopic transport-model calculations to explore possible deviation from the ideal m_T-scaling especially in order to understand "non-Gaussian" effects as well as the HBT puzzles.

In this Letter, we investigate the m_T dependence of the HBT parameters with three kinds of identical-particle correlations: $\pi^- - \pi^-$, $K^+ - K^+$, and $\Lambda - \Lambda$. So far the majority of HBT investigations are on the $\pi - \pi$ pairs due to their large yield. In order to obtain a cleaner signal with sensitivity to earlier stages of HICs, kaon–kaon correlations have been explored at several energies [4,21–24]. Besides mesons, in order to map out a widespread m_T-dependence, the $\Lambda - \Lambda$ baryonic correlation is the next convenient choice. It is an identical non-charged-particle correlation so that a similarly Gaussian shape as for pions can be expected if the nuclear potential is not considered in FSI.

To explore the m_T-scaling, we employ the UrQMD model. In UrQMD, the hadrons are represented by Gaussian wave packets in phase space. After the Wood–Saxon initialization, the phase space of hadrons is propagated according to Hamilton's equation of motion [25,26], $\dot{\mathbf{r}}_i = \frac{\partial H}{\partial \mathbf{p}_i}$ and $\dot{\mathbf{p}}_i = -\frac{\partial H}{\partial \mathbf{r}_i}$. Here $\mathbf{r}_i$ and $\mathbf{p}_i$ are the coordinate and the momentum of hadron i. The Hamiltonian H consists of the kinetic energy T and the effective interaction potential energy U, $H = T + U$. The two-body Coulomb potential is considered for formed charged particles. Recently, a soft equation of state with momentum dependence (SM-EoS) for formed hadrons and a density dependent Skyrme-like term for "pre-formed" hadrons from string fragmentation have been supplied into the UrQMD transport model, please see details in [13,27]. For observables such as the nuclear stopping, the elliptic flow and the HBT parameters of pions visible improvement towards the data has been observed if these potentials are included. Especially, the HBT "t-puzzle" for pions can be consistently solved. In this Letter, we continue this topic and further calculate the HBT parameters of kaon and Λ sources.

Three cases of experimental data at mid-rapidity are compared with our calculations and the phase space cuts are the same as those listed in [7], the three systems under investigation are: (1) central Pb + Pb collisions at the SPS beam energy $E_{lab} = 20\,A$ GeV, (2) central Pb + Pb collisions at the SPS beam energy $E_{lab} = 158\,A$ GeV, (3) central Au + Au collisions at the top RHIC energy $\sqrt{s_{NN}} = 200$ GeV. For each case about 25 thousand central events are calculated. If not stated otherwise, the UrQMD transport program stops at $t_{cut} = 200$ fm/c, the residual long-lived unstable resonances are forced not to decay after this final cut time. All particles with their phase space coordinates at their respective freeze-out time t_f (last collisions) are put into the analyzing program to be discussed below. When studying the time-evolution of the particle correlation (shown in Fig. 4), we produce output at $t_{cut} = 5, 10, 15, 20, 25, 50,$ and 75 fm/c, separately, while other parameters are not altered.

The "correlation after-burner" (CRAB v3.0β) program [28,29] is then adopted for analyzing the interactions of two particles after freeze-out with quantum statistics and final state modifications so that one can construct the HBT correlator to be compared with experimental data. In this work, the strong interaction of pions and kaons is not considered in FSI because of its negligible effect [30]. However, we also noticed that the effect of strong FSI influences the final HBT results of neutral K_s^0 source [23]. For Λs, the nuclear modification is not considered in this work for simplicity. We will, however, briefly discuss this issue in Fig. 3. Concerning the contribution of the final state Coulomb interaction to the correlator, it is checked for the charged pion–pion and kaon–kaon cases. One billion pairs are performed at mid-rapidity of single or two correlated particles as stated in [7] in each CRAB analyzing run.
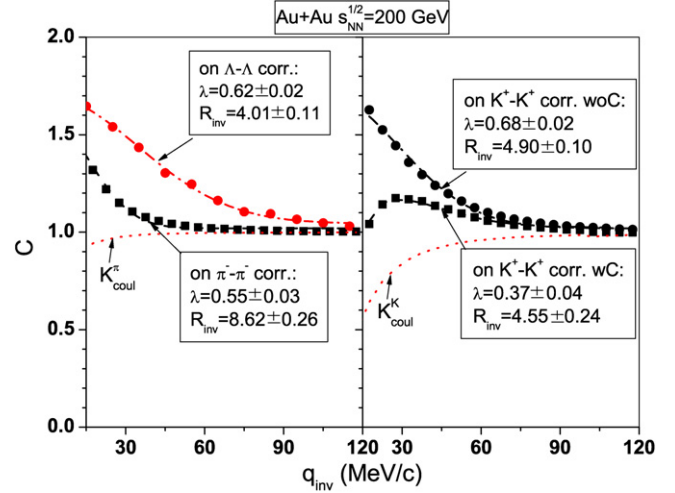

Fig. 1. One-dimensional invariant correlation function for pion, Λ, and kaon sources for central Au + Au reactions at $\sqrt{s_{NN}} = 200$ GeV. The potentials for both "pre-formed" and formed particles are considered in calculations. In the left plot: The squares and circles represent the calculation results for pion and Λ source without modifications on FSI, separately. The dashed and dash-dotted lines are the fitting results to them. In the right plot: The squares and circles represent the calculation results for kaon source with and without Coulomb modification, separately. The dashed and dash-dotted lines are the fitting results to them. The Coulomb correction factors of $\pi^- - \pi^-$ and $K^+ - K^+$ pairs (K^π_{coul} and K^K_{coul}) are also shown in both plots by thin dotted lines.

In the next step, we fit the correlator as a three-dimensional Gaussian form under the Pratt convention (using ROOT [31] and the χ-squared method), i.e., the longitudinally co-moving system (LCMS). When the nuclear and Coulomb modifications are not considered in the correlator, the fitting function can be expressed in the standard way,

$$C(q_L, q_O, q_S) = 1 + \lambda e^{-R_L^2 q_L^2 - R_O^2 q_O^2 - R_S^2 q_S^2 - 2R_{OL}^2 q_O q_L}. \tag{1}$$

In Eq. (1), λ is normally referred to as an incoherence factor. It might be also affected by many other factors, such as the contaminations, long-lived resonances, or the details of the Coulomb modification in FSI. Thus, we regard it as a free parameter. R_L, R_O, and R_S are the Pratt radii in longitudinal, outward, and sideward directions, while the cross-term R_{OL} plays a role at large rapidities. q_i is the pair relative momentum $\mathbf{q}$ ($\mathbf{q} = \mathbf{p}_1 - \mathbf{p}_2$) in the i direction.

If one considers the Coulomb effect in FSI for charged-particle pairs, a Bowler–Sinyukov method, which has been used in STAR experiments [30], can be exploited in the fitting process:

$$\begin{aligned} &C(q_L, q_O, q_S) \\ &= (1 - \lambda) + \lambda K_{coul}(q_{inv})\left(1 + e^{-R_L^2 q_L^2 - R_O^2 q_O^2 - R_S^2 q_S^2 - 2R_{OL}^2 q_O q_L}\right), \end{aligned} \tag{2}$$

where the K_{coul} is the Coulomb correction factor and depends only on q_{inv} as same as experiments. The $q_{inv} = \sqrt{\mathbf{q}^2 - (\Delta E)^2}$ is the invariant relative momentum, where $\Delta E = E_1 - E_2$ is the energy difference of two particles.

Fig. 1 shows the one-dimensional invariant correlation function for pion (left plot), Λ (left plot), and kaon (right plot) sources for central Au + Au reactions at $\sqrt{s_{NN}} = 200$ GeV. A transverse momentum, k_T, cut is not applied. The pairs are binned with $\Delta q_{inv} = 5$ MeV/c for pions and kaons while $\Delta q_{inv} = 10$ MeV/c for Λs due to the small yield of Λs in each event. The upper limit is $q_{inv} = 120$ MeV/c. The pairs within $\mathbf{q} < 5$ MeV/c are not used for fitting due to the large errors from split and merged tracks in the experiments. The left plot shows that the Gaussian parameterization is still suitable for pion–pion and $\Lambda - \Lambda$ correlators if strong and Coulomb modifications are not considered in FSI. It was found
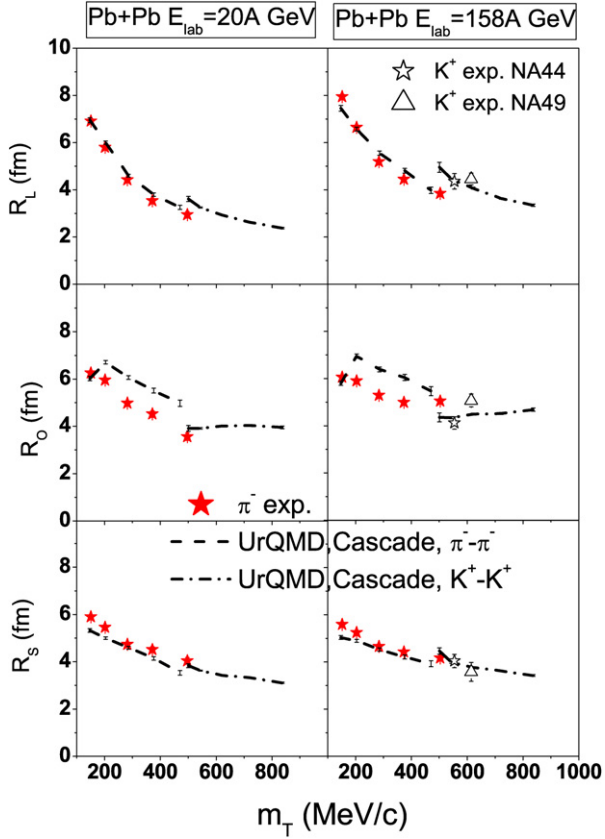
Fig. 2. m_T-dependence of the HBT radii of π^- (dashed lines) and K^+ (dash-dotted lines) sources in central Pb + Pb collisions for $E_{lab} = 20\,A$ GeV (left plots) and $E_{lab} = 158\,A$ GeV (right plots) cases (with the cascade mode in UrQMD calculations). The experimental NA49 and NA44 data of pions and kaons are also shown by solid and open symbols, separately [21,24,36].

Fig. 3. m_T-dependence of the HBT radii of π^- (dashed lines), K^+ (dash-dotted lines), and Λ (dash-dot-dotted lines) sources in central Au + Au collisions at $\sqrt{s_{NN}} = 200$ GeV with potentials only for formed baryons (left plots) and with potentials for both formed baryons and "pre-formed" particles (right plots). The experimental RHIC data of pions and kaons are shown by solid and open stars separately [22,30,35]. The function $R_i = 3/\sqrt{m_T}$ is also shown by solid line in each plot.

that the Coulomb correction factor influences the correlator of pions at $q_{inv} \lesssim 30$ MeV/c [14,32] which is supported by the present calculation as indicated by the flat K_{coul}^π (thin dotted line). It is also found that the K_{coul}^π factor in Eq. (2) reduces the final HBT radii of pion source only slightly at $k_T \lesssim 100$ MeV/c, while the reduction of λ is about 0.1. A similar effect of Coulomb modification on the HBT radii and the λ factor was also observed in previous calculations [33,34]. The one-dimensional fitting results (R_{inv}) for pions and Λs show that the pion's homogeneity length is about twice larger than for Λs, which implies that more Λs are emitted from the early stage. In addition, the larger λ factor indicates that Λs are less affected by the decay of resonances at late stage, although some amount of Λs are produced by the decay of Σ^* resonances. Fig. 1 (right) shows the R_{inv} of the K^+ source which lies between that of the pion and Λ source, also the λ value of the kaon source is largest, which supports that kaons are produced earliest among the investigated particles [25]. However, for kaons, the Coulomb modification alters the correlator up to the large value of q_{inv}, ~ 60 MeV/c. Although a strong reduction of the R_{inv} is not seen, λ is reduced by ~ 0.3. The Coulomb corrected λ values of pions and kaons match the data much better [22,30, 35]. Due to the fact that the Coulomb modification to the kaon–kaon correlation is larger than for the pion–pion correlation, we adopt the Bowler–Sinyukov fitting method expressed in Eq. (2) after constructing the 3-dimensional correlator of kaon source with Coulomb modifications.

The HBT parameters can be as a function of m_T, where $m_T = \sqrt{k_T^2 + m^2}$ where m is the pion, kaon, or Λ mass and $\mathbf{k}_T = (\mathbf{p}_{1T} + \mathbf{p}_{2T})/2$ is the transversal component of the average momentum $\mathbf{k}$
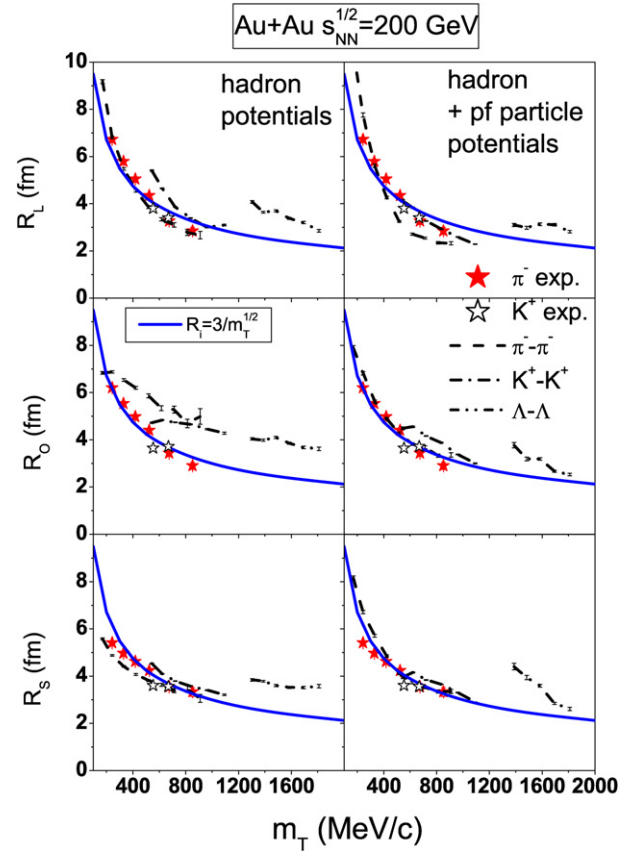
of two particles, $\mathbf{k} = (\mathbf{p}_1 + \mathbf{p}_2)/2$. Fig. 2 depicts the calculated m_T-dependence of the HBT radii R_L (top plots), R_O (middle plots), and R_S (bottom plots) of π^- (dashed lines) and K^+ (dash-dotted lines) sources in central Pb + Pb collisions at $E_{lab} = 20\,A$ GeV (left plots) and at $E_{lab} = 158\,A$ GeV (right plots). The cascade results are compared with data (solid stars for pion data at both beam energies [36], open symbols for kaon data at 158 GeV from the NA44 and the NA49 Collaborations [21,24]). One should bear in mind that the kaon data are obtained under slightly different physical cuts from the pion case. For instance, in Ref. [24], the 5% most central interactions are selected for the central kaon data sample while the 7.2% most central interactions are selected for pions [36]. At $E_{lab} = 20\,A$ GeV, we observe m_T-scaling for pions and kaons in R_L and R_S, only the calculated R_O of the pion source is slightly larger than the data. It is also seen that the m_T-dependence of R_O of the kaon source is weak. At $E_{lab} = 158\,A$ GeV, the m_T-scaling of R_S and R_L still hold with similar problems for R_O. However, one should note that the few currently available kaon data cannot sufficiently evaluate the performance of the scaling.

Let us move on to see the m_T-dependence of HBT radii of pions (dashed lines), kaons (dash-dotted lines), and Λs (dash-dot-dotted lines) at the top RHIC energy $\sqrt{s_{NN}} = 200$ GeV, which is shown in Fig. 3. The pion data (solid stars) are from [30,35], and the preliminary kaon data (open stars) are from [22]. The left plots show the calculations with the SM-EoS for formed baryons, while the calculations with potentials for both "pre-formed" and formed particles are shown in the right plots. In each plot, the m_T-scaling function $R_L = R_O = R_S = 3/\sqrt{m_T}$ is also shown by solid line. In Fig. 3

(left), one cannot observe m_T-scaling in all HBT directions if the potentials are considered only for formed baryons. Although the calculated R_S of kaons stay on the scaling line, those of Λs are about 1.2 fm above the scaling line. Further, R_L values of kaons and Λs are larger than the scaling results. In the R_O direction the same is true for the HBT radii of pions, kaons and Λs. Let us now consider potentials for "pre-formed" hadrons as discussed in [13]. Fig. 3 (right) shows that the transverse radii R_O and R_S of the pion source nicely follow the scaling line. However, a steeper m_T-dependence of R_L is seen which might be due to the absence of a proper collision term for the "pre-formed" hadrons. Secondly, it is exciting to see that the "pre-formed" hadron potential leads to a smaller R_L (R_O) of kaon pairs as well so that the HBT radii of kaons also follow the scaling line quite well. Thirdly, the results for Λs also approach towards the scaling line especially at large k_T where the effect of resonance decay is minor because of an early emission. At small k_T, the decay of long-lived resonance $\Sigma(1385)$ into Λs enlarges the HBT radii. Meanwhile, the absence of the nuclear modification on FSI might also play a role, which deserves a further investigation.

Based on discussions in Figs. 1–3, we conclude that interactions at the late stage (including the modifications in FSI) indeed influences the HBT parameters. The idea of "pre-formed" hadron interactions does not only solve the HBT "time (R_O/R_S)-puzzle", but also improves the m_T-scaling considerably. To elaborate further on this point, Fig. 4 shows the time evolution of the ratio R_O/R_S and the incoherence factor λ of pion pairs at $250 < k_T < 350$ MeV/c for central Au+Au reactions at $\sqrt{s_{NN}} = 200$ GeV. Calculations with and without "pre-formed" hadron potential are compared. The corresponding experimental data of the R_O/R_S and λ are indicated by a square and a circle at the right end of the plot. Without "pre-formed" particle interactions, the R_O/R_S ratio increases rapidly up to $t \sim 25$ fm/c from ~ 1.0 to ~ 1.5. In contrast, considering the "pre-formed" hadron potential, the ratio R_O/R_S is nearly time independent (stays at its start value of $R_O/R_S \sim 1 \pm 0.05$). The effects of FSI continue to play visible roles (although relatively weakly after 25 fm/c) on the λ factor, which is also consistent with the visible suppressing effect of the Coulomb modification of FSI on the λ value from the analysis of Fig. 1. We also find that the "pre-formed" hadron potential reduces the λ further to approach the data.

For central collisions, the HBT radii can be (approximately) analytically obtained under the assumptions of thermalization and Gaussian-source shape and be expressed as [14,37],

$$R_L^2 = \langle (\tilde{z} - \beta_L \tilde{t})^2 \rangle, \tag{3a}$$

$$R_O^2 = \langle (\tilde{x} - \beta_T \tilde{t})^2 \rangle, \tag{3b}$$

$$R_S^2 = \langle \tilde{y}^2 \rangle. \tag{3c}$$

Here the space–time coordinates $\tilde{x}$, $\tilde{y}$, $\tilde{z}$, and $\tilde{t}$ are relative distances to their "effective source centers" ($\bar{x}^\mu = \langle x^\mu \rangle$): $\tilde{x}^\mu = x^\mu - \bar{x}^\mu$. And β_L and β_T are components of the velocity of particle pair β ($\beta = \mathbf{k}/k^0$, $k^0 = (E1 + E2)/2 \approx \sqrt{m^2 + \mathbf{k}^2}$ is the average energy of two particles. Usually, the on-shell approximation is used). Eq. (3b) can also be expanded as

$$R_O^2 = \langle \tilde{x}^2 \rangle + \langle \beta_T^2 \tilde{t}^2 \rangle - 2 \langle \beta_T \tilde{x} \tilde{t} \rangle. \tag{4}$$

In central collisions, because of the longitudinal reflection symmetry, $\langle \tilde{x}^2 \rangle \simeq \langle \tilde{y}^2 \rangle$. Therefore, by comparing Eq. (3c) with Eq. (4), it is clear that the difference of R_O and R_S mainly comes from the relative strength of the time-related term $\langle \beta_T^2 \tilde{t}^2 \rangle$ and the $\tilde{x}$–$\tilde{t}$ correlation term $-2 \langle \beta_T \tilde{x} \tilde{t} \rangle$. Thus, one obtains a clear interpretation of the large reduction of the R_O/R_S ratio (even $R_O/R_S < 1$ may happen), if "pre-formed" particle interactions are taken into account
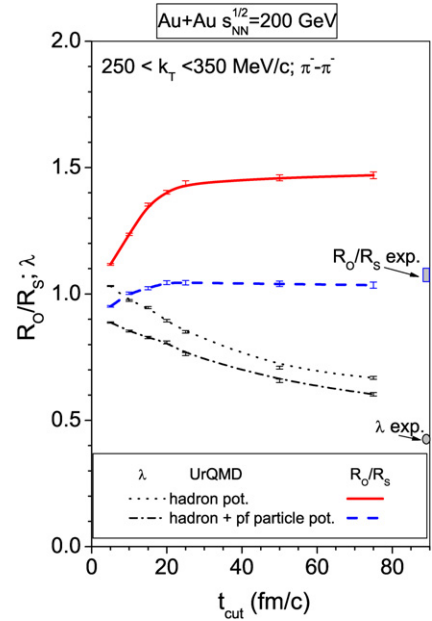

Fig. 4. Time evolution of the ratio R_O/R_S and the λ factor of pion source at $250 < k_T < 350$ MeV/c, which are calculated with potentials for formed baryons and with potentials for both formed and "pre-formed" particles, are shown by different lines. The R_O/R_S and λ experimental data are represented by a square and a circle at the right end of the plot.
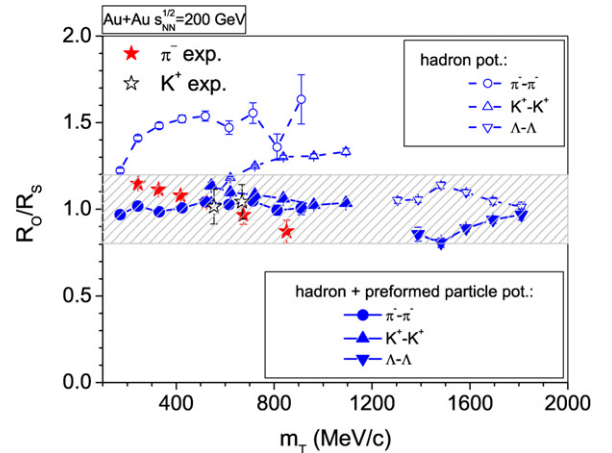

Fig. 5. m_T-dependence of the ratio R_O/R_S of π^-, K^+, and Λ sources for Au + Au reactions at $\sqrt{s_{NN}} = 200$ GeV with potentials only for formed baryons (lines with open symbols) and with potentials for both formed and "pre-formed" particles (lines with solid symbols). Solid and open stars represent the RHIC data of pions and kaons separately [22,30,35]. A 20% deviation margin is marked in light gray.

by relating it to the stronger phase-space correlation induced by the potentials.

Fig. 5 shows the m_T-dependence of the ratio R_O/R_S of π^-, K^+, and Λ sources at transverse momenta $250 < k_T < 350$ MeV/c for central Au + Au reactions at $\sqrt{s_{NN}} = 200$ GeV. The calculations with potentials only for formed baryons (lines with open symbols) and with potentials for both formed and "pre-formed" particles (lines with solid symbols) are compared with pion data [30,35] and preliminary kaon data [22]. Considering the uncertainties from the non-Gaussian effect [16] as well as the variant treatments of Coulomb correction on FSI (see [30,32]), a 20% deviation margin is marked in light gray. It is seen that, although the effect of the formed hadron potentials on the ratio becomes weaker with the increase of particle mass, the R_O/R_S values of pions and kaons at large k_T are above the upper limit of the shadowed area. The

inclusion of "pre-formed" particle interactions cures these deviations and allows for a consistent understanding of the data. Here it should be addressed that due to the $\tilde{x}$–$\tilde{t}$ correlation shown in Eq. (4), the $R_O/R_S \to 1$ does not mean that the mean duration time should approach zero, a finite non-zero mean proper duration time has been discovered by recent experiments [18] via three-dimensional source imaging methods which definitely deserve further transport-model analysis.

To summarize, the m_T dependence of the HBT parameters for pion, kaon, and Λ sources are investigated at three SPS and top RHIC energies with a microscopic transport model (UrQMD). In the cascade mode (i.e., without potential interactions), the HBT radii R_L and R_S fall roughly with the m_T-scaling only at the lowest SPS energy $E_{\text{lab}} = 20\,A$ GeV, while the R_O at all energies and the R_L at energies $E_{\text{lab}} = 158\,A$ GeV and $\sqrt{s_{NN}} = 200$ GeV are apart from the m_T-scaling line. Even the inclusion of potentials for formed hadrons does not alter this picture. However, with a density dependent potential for "pre-formed" particles from string fragmentation, the HBT radii of pion and kaon sources, even those of the Λ source, are seen to follow the m_T-scaling line $R = 3/\sqrt{m_T}$ fairly well. The strong and Coulomb interactions at late stage are observed to influence the HBT radii and the λ factor. The HBT "t-puzzle" in many calculations exhibited by the larger R_O/R_S ratios of pion and kaon sources than data can only be solved by the "pre-formed" hadron potential which dominates *at the early stage* of HICs.

Acknowledgements

References

[1] D.H. Rischke, M. Gyulassy, Nucl. Phys. A 608 (1996) 479.
[2] J.W. Harris, Int. J. Mod. Phys. E 16 (2007) 643.
[3] J. Adams, et al., STAR Collaboration, Nucl. Phys. A 757 (2005) 102.
[4] M.A. Lisa, S. Pratt, R. Soltz, U. Wiedemann, Annu. Rev. Nucl. Part. Sci. 55 (2005) 357.
[5] Q. Li, M. Bleicher, H. Stoecker, Phys. Rev. C 73 (2006) 064908.
[6] Q. Li, M. Bleicher, X. Zhu, H. Stoecker, J. Phys. G 33 (2007) 537.
[7] Q. Li, M. Bleicher, H. Stoecker, J. Phys. G 34 (2007) 2037.
[8] Z. Lin, C.M. Ko, S. Pal, Phys. Rev. Lett. 89 (2002) 152301.
[9] J.G. Cramer, G.A. Miller, J.M.S. Wu, J.H.S. Yoon, Phys. Rev. Lett. 94 (2005) 102302;
J.G. Cramer, G.A. Miller, J.M.S. Wu, J.H.S. Yoon, Phys. Rev. Lett. 95 (2005) 139901, Erratum.
[10] T.J. Humanic, Int. J. Mod. Phys. E 15 (2006) 197.
[11] P. Romatschke, Eur. Phys. J. C 52 (2007) 203.
[12] S. Pratt, arXiv: 0710.5733 [nucl-th].
[13] Q. Li, M. Bleicher, H. Stocker, Phys. Lett. B 659 (2008) 525.
[14] U.A. Wiedemann, U.W. Heinz, Phys. Rep. 319 (1999) 145.
[15] R.A. Lacey, Braz. J. Phys. 37 (2007) 893.
[16] P. Chung, P. Danielewicz, NA49 Collaboration, J. Phys. G 34 (2007) S1109.
[17] P. Danielewicz, S. Pratt, Phys. Rev. C 75 (2007) 034907.
[18] S. Afanasiev, PHENIX Collaboration, arXiv: 0712.4372 [nucl-ex].
[19] Z. Lin, C.M. Ko, J. Phys. G 30 (2004) S263.
[20] T. Csorgo, B. Lorstad, Phys. Rev. C 54 (1996) 1390.
[21] I.G. Bearden, et al., NA44 Collaboration, Phys. Rev. Lett. 87 (2001) 112301.
[22] S. Bekele, STAR Collaboration, J. Phys. G 30 (2004) S229.
[23] B.I. Abelev, et al., STAR Collaboration, Phys. Rev. C 74 (2006) 054902.
[24] S.V. Afanasiev, et al., Phys. Lett. B 557 (2003) 157.
[25] S.A. Bass, et al., UrQMD Collaboration, Prog. Part. Nucl. Phys. 41 (1998) 255.
[26] M. Bleicher, et al., UrQMD Collaboration, J. Phys. G: Nucl. Part. Phys. 25 (1999) 1859.
[27] Q. Li, M. Bleicher, H. Stöcker, in preparation.
[28] S. Pratt, et al., Nucl. Phys. A 566 (1994) 103C.
[29] S. Pratt, CRAB version 3, http://curly.pa.msu.edu/~scottepratt/freecodes/crab/home.html.
[30] J. Adams, et al., STAR Collaboration, Phys. Rev. C 71 (2005) 044906.
[31] http://root.cern.ch/.
[32] D. Adamova, et al., CERES Collaboration, Nucl. Phys. A 714 (2003) 124.
[33] D. Hardtke, T.J. Humanic, Phys. Rev. C 57 (1998) 3314.
[34] S. Pratt, Phys. Rev. D 33 (1986) 72.
[35] S.S. Adler, et al., PHENIX Collaboration, Phys. Rev. Lett. 93 (2004) 152302.
[36] S. Kniege, et al., NA49 Collaboration, AIP Conf. Proc. 828 (2006) 473.
[37] M. Herrmann, G.F. Bertsch, Phys. Rev. C 51 (1995) 328.